JOURNAL OF MATERIALS SCIENCE 33 (1998) 385–394

Effects of Cu addition on the β-phase formation rate in Fe_2Si_5 thermoelectric materials

I. YAMAUCHI, H. OKAMOTO*, A. SUGANUMA*, I. OHNAKA
Department of Material Science and Processing, Osaka University, 2-1, Yamadaoka, Suita, Osaka 565, Japan

We proposed Fe_2Si_5 based alloys with a small amount of Cu as new Fe–Si thermoelectric materials. A few acicular structures enriched in Cu were newly formed in slowly solidified alloys containing Cu above 0.2 at %. α single phase structure was formed by a conventional solidification process in alloys below 0.2 at % Cu. β phase was only formed by the eutectoid reaction ($\alpha \rightarrow \beta + Si$). Differential thermal analysis, X-ray diffraction and structure observation clearly confirmed that the eutectoid reaction rate was drastically enhanced by the addition of a small amount of Cu and its rate decreased with decrease of Cu content. Its rate also depended on the annealing temperature and it was maximum at about 1073 K for most alloys. The addition of only 0.1 at % Cu was still very effective in Mn or Co doped alloys. The final structure after the eutectoid reaction in these alloys was duplex composed of β and Si. The size of Si decreased with decrease of Cu content and the annealing temperature. Transmission electron microscope observation showed that β was transformed from α with many planar faults (stacking fault) that will act as a drag resistance for the transformation. We speculated that the addition of Cu probably decreased the stacking fault energy so as to decrease the drag force and to enhance the formation rate.

1. Introduction

The β-$FeSi_2$ alloy is known as an excellent high thermoelectric material which can be used in high temperature air atmosphere [1–3]. An alloy with $FeSi_2$ composition will solidify as a eutectic composed of α and ε from an equilibrium Fe–Si alloy phase diagram (Fig. 1) [4]. These phases are metallic and they show low thermoelectric power. The alloy should be annealed to get a single β which is a semiconductor phase showing a high thermoelectric power. The coarse eutectic structure is usually formed in conventional casting processes because of its low solidification rate. The β formation rate by the peritectoid reaction ($\alpha + \varepsilon \rightarrow \beta$) is slow and it takes a long time (more than 100 h) to get complete β, especially in alloys with coarse eutectic structures, because the peritectoid reaction rate is controlled by the diffusion through the newly formed solid β layer [5, 6]. On the other hand, the β formation from α by the eutectoid reaction ($\alpha \rightarrow \beta + Si$) is essentially independent of the size of α.

We reported that a small amount of Cu addition drastically enhanced the β formation rate in various $FeSi_2$ composition alloys [7]. Some extent of the enhancement was owing to the increase of the peritectoid reaction rate by Cu addition. However, that was limited to the initial stage of that reaction. As a result, Cu addition was not so effective in decreasing the total time for the complete elimination of coarse ε by the peritectoid reaction [7]. As long as we select $FeSi_2$ composition alloy, it will be difficult to neglect the existence of coarse ε for the complete β formation. Such retained metallic ε will decrease the thermoelectric power owing to form an electrical circuit.

It is interesting to apply alloys with the composition of Fe_2Si_5 instead of $FeSi_2$. In this alloy, ε was not formed, therefore such problems will be eliminated. However, there have been few papers on this composition alloy. In this paper, we examined effects of Cu on the β formation rate and its structure change during the annealing by the differential thermal analysis, X-ray diffraction, structure observation by the scanning electron microscopy and the transmission electron microscopy.

2. Experimental procedure

Various binary Fe_2Si_5 and Fe_2Si_5–(Cu,Mn,Co) alloys listed in Table I were used. They were prepared from 99.9 mass % electrolytic iron, high purity Si for semiconductor, 99.9 mass % electrolytic Mn, Co and Cu. They were melted in an aluminium crucible under Ar gas atmosphere. The molten metal was cast into a quartz tube of 4 mm in diameter by a vacuum

* Formerly undergraduate student of Osaka University.
Present address: Kurimoto Ltd. Kagaya Factory, 1-64, Izumi 2-chome, Suminoe-ku, Osaka 559, Japan

0022–2461

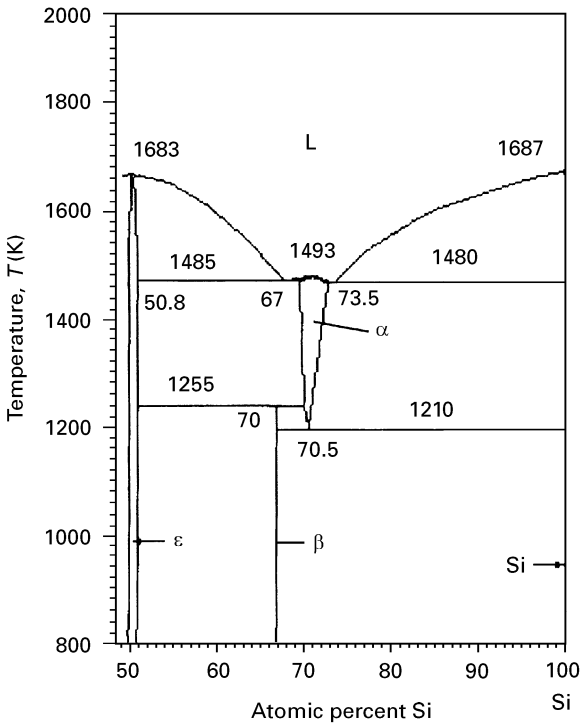

Figure 1 Equilibrium phase diagram of Fe–Si system.

TABLE I Nominal alloy composition (at %)

Alloy	Fe	Si	Mn	Co	Cu
Fe_2Si_5	28.19	71.81	–	–	–
Fe_2Si_5–0.1Cu	28.14	71.76	–	–	0.1
Fe_2Si_5–0.2Cu	28.12	71.68	–	–	0.2
Fe_2Si_5–0.5Cu	28.03	71.47	–	–	0.5
Fe_2Si_5–1.0Cu	28.00	71.00	–	–	1.0
$Fe_2Si_5$1Mn	28.00	71.00	1.0	–	–
$Fe_2Si_5$1Mn–0.1Cu	27.86	71.04	1.0	–	0.1
$Fe_2Si_5$1Mn–0.2Cu	27.83	70.97	1.0	–	0.2
$Fe_2Si_5$1Mn–0.5Cu	27.75	70.75	1.0	–	0.5
$Fe_2Si_5$1Mn–1.0Cu	27.50	70.50	1.0	–	1.0
$Fe_2Si_5$1Co	28.00	71.00	–	1.0	–
$Fe_2Si_5$1Co–0.1Cu	27.86	71.04	–	1.0	0.1
$Fe_2Si_5$1Co–0.2Cu	27.83	70.97	–	1.0	0.2
$Fe_2Si_5$1Co–0.5Cu	27.75	70.75	–	1.0	0.5
$Fe_2Si_5$1Co–1.0Cu	27.50	70.50	–	1.0	1.0

suction method. As-solidified structures were observed by BEI (back-scattered electron image) of the scanning electron microscope (SEM) without etching. The cyclic heating and cooling experiments between 873 and 1323 K were carried out by using a microthermal differential analysis (DTA) to examine the transformation behaviour. The heating or cooling rate in DTA was 0.25 K s^{-1}. The temperature range in those experiments involved the equilibrium eutectoid temperature, as shown in Fig. 1. The isothermal annealing for the β formation was carried out at various temperatures between 873 and 1173 K for a given period in vacuum atmosphere. The structure change with the heat treatment was also observed by SEM and X-ray diffraction (XRD). Some specimens were observed by transmission electron microscopy (TEM) after the chemical polishing by using a similar solution described in Sumida *et al.* [8].

3. Experimental results and discussion

3.1. Effects of Cu addition on the solidified structure

Fig. 2a and b shows the as-solidified structure of binary Fe_2Si_5 and $Fe_2Si_5$1Co alloys. There was no significant difference between them. The structure seemed to be a single phase. Some dark streaks were observed in both specimens. They were cracks that

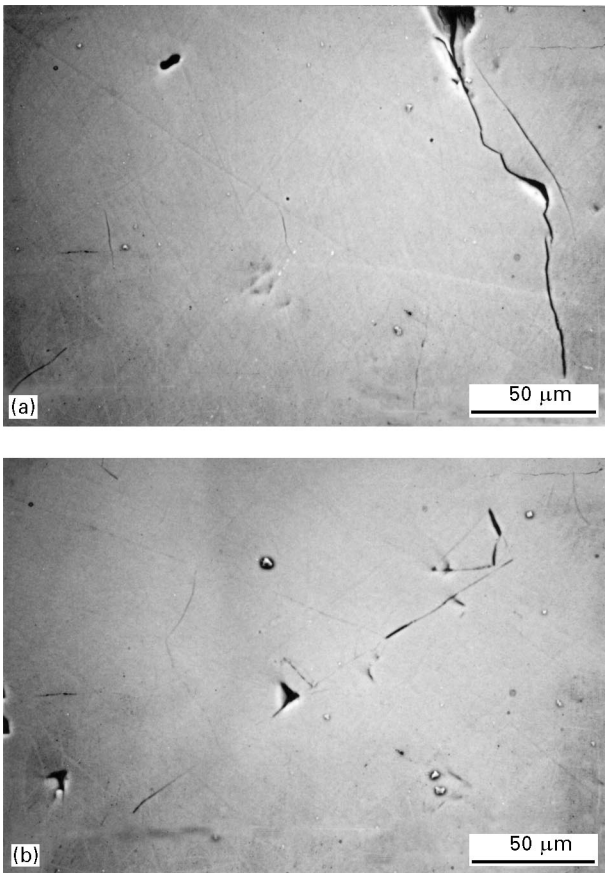

Figure 2 Microstructure of (a) Fe_2Si_5 and (b) $Fe_2Si_5$1Co (slowly solidified).

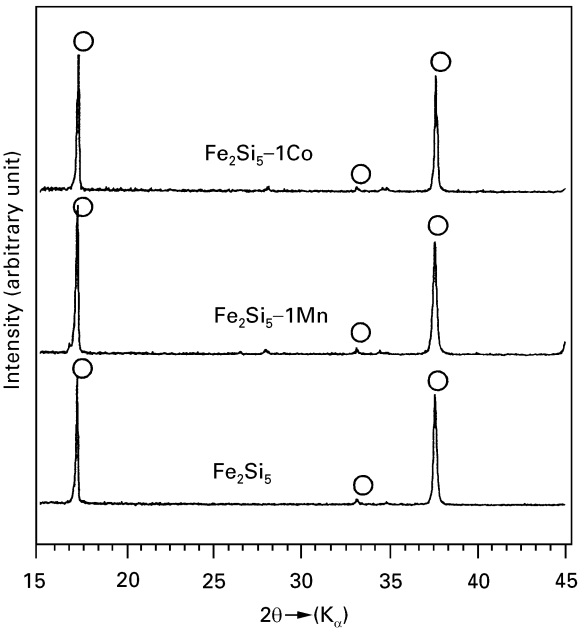

Figure 3 Effect of dopant on X-ray diffraction patterns of as-solidified specimens. (○) α.

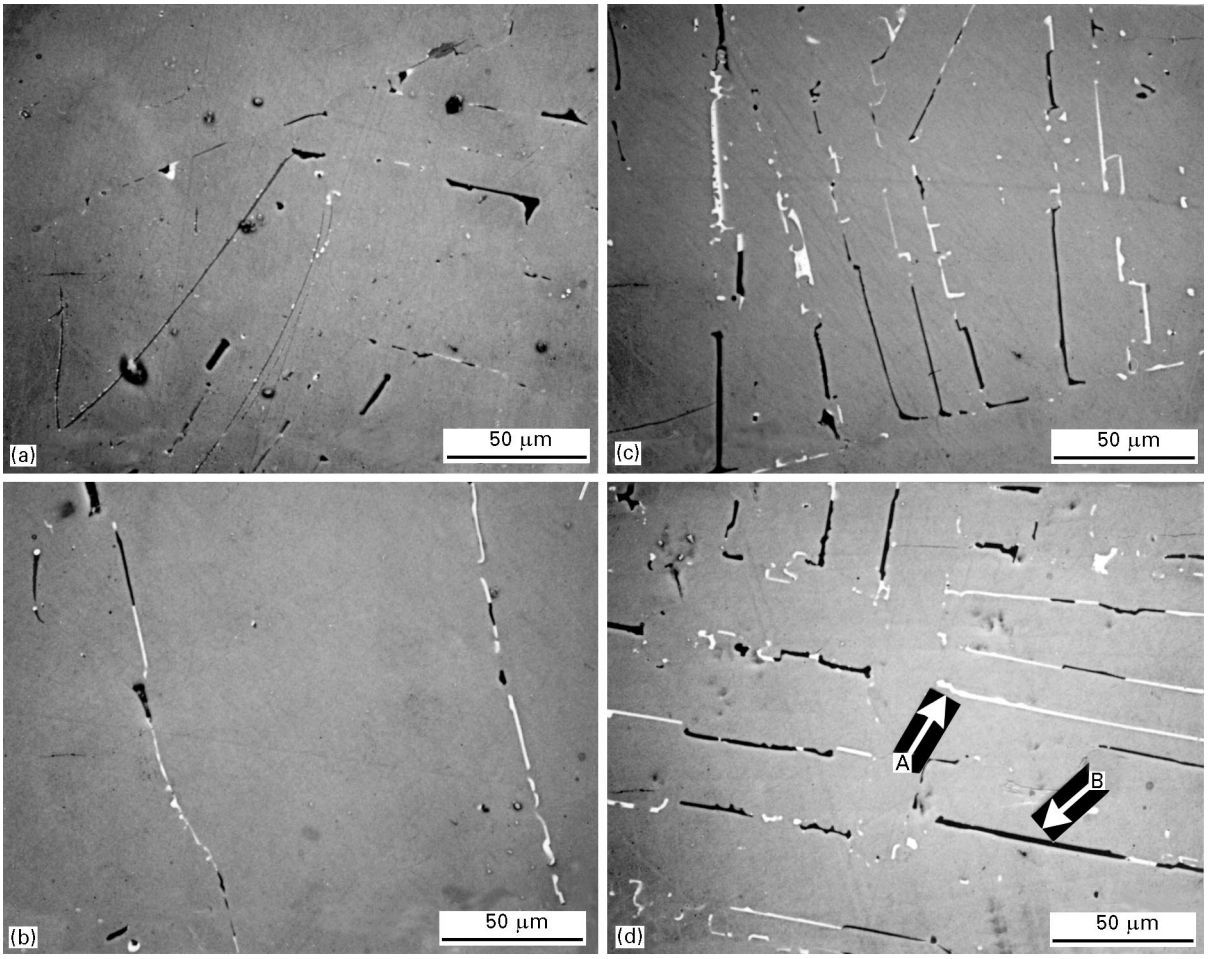

Figure 4 Effect of Cu content on as-solidified structure of Fe_2Si_51Mn–XCu alloys, (a) 0.1 at % Cu; (b) 0.2 at % Cu; (c) 0.5 at % Cu; (d) 1.0 at % Cu.

TABLE II Results of EPMA analysis of slowly solidified Fe_2Si_5–1Cu alloy (mean value at %)

Phase	Fe	Si	Cu
α	29.0 (± 1.5)	70.0 (± 1.5)	< 0.5
White streak (Cu rich)	5.8 (± 1)	22.9 (± 2)	71.3 (± 1)
Dark streak (Si rich)	11.5 (± 1)	88.5 (± 1)	< 0.2

were probably generated during the solidification, or cooling after solidification. The structure of Fe_2Si_51Mn alloy was also similar to the above.

Fig. 3 shows X-ray diffraction patterns of these specimens. They were essentially similar. There was no other detectable diffraction lines except those of α. One atomic percent of Mn or Co was completely dissolved in the binary Fe_2Si_5 alloy.

Fig. 4a–d shows the effect of Cu on the solidification structure in Fe_2Si_5 alloys. These structures were also almost same as those of Mn or Co added alloys. We can see several streaks in Cu added alloys above 0.2 at % (shown by arrows A and B in Fig. 4d). These streaks are composed white and dark parts. The white and dark parts were enriched in Cu and Si, respectively. There is no Cu rich phase in 0.1 Cu added alloy as shown in Fig. 4a. That composition obtained by electron probe microanalysis (EPMA) is shown in Table II. The solubility of Cu in α was quite too low to evaluate the exact Cu content by EPMA but the

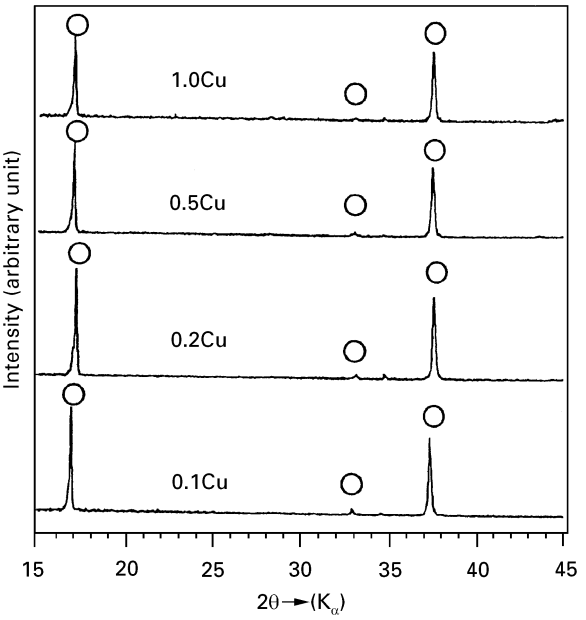

Figure 5 Effect of Cu content on X-ray diffraction patterns of as-solidified Fe_2Si_51Mn alloys. (○) α.

solubility in slowly solidified state may qualitatively be among 0.1 and 0.2% Cu by structure observation.

The equilibrium phase diagram of Fe–Si binary system [4] suggests that Si streaks were probably formed at the final stage of solidification. Cu was

rejected from α during the solidification and enriched in liquid. From the similarity of the solidification morphology to that of Si, Cu enriched liquid probably solidified at the final stage. If the dissolved Cu in α is only effective to enhance the eutectoid decomposition of α to β + Si, it is possible to decrease Cu content to 0.2 at %. Elongated structural morphology of Cu-enriched phase is harmful for the high thermoelectric material because such a metallic phase forms an electric short circuit to lead a low thermo-electric power.

Fig. 5 shows an example of X-ray diffraction patterns of various as-solidified Fe_2Si_51Mn–X Cu alloys.

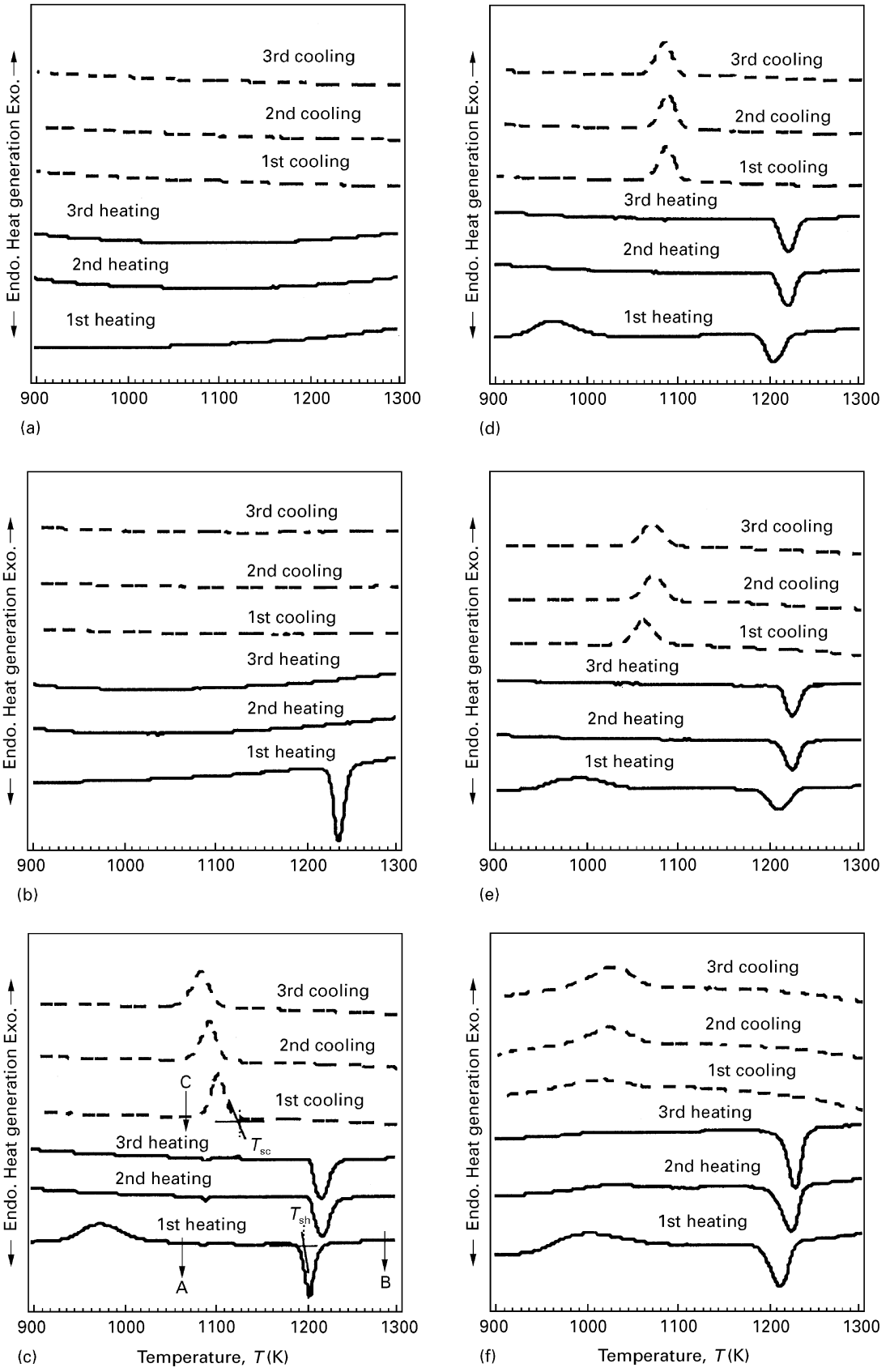

Figure 6 Effect of Cu content on cyclic DTA curves of Fe_2Si_51Mn–XCu alloys. (a) Fe_2Si_51Mn; (b) Fe_2Si_51Mn preannealed at 973 K for 5.28×10^4 s; (c) Fe_2Si_51Mn–1Cu; (d) Fe_2Si_51Mn–0.5Cu; (e) Fe_2Si_51Mn–0.2Cu; (f) Fe_2Si_51Mn–0.1Cu.

There were no significant differences between them. Some diffraction lines of α were only observed and it was difficult to detect lines from Cu and Si enriched phases shown in Fig. 4 owing to few quantities of them.

3.2. DTA measurements of Fe_2Si_5 alloys and the effect of Cu on them

Fig. 6 shows typical DTA curves in various $Fe_2Si_5$1Mn–XCu alloys. There are no exothermic or endothermic peaks in a Cu free alloy (Fig. 6a). It means that reactions such as $\alpha \rightarrow \beta + Si$ or $\beta + Si \rightarrow \alpha$ has not occurred during the DTA measurements in this alloy. The α in as-solidified state of this alloy was quite stable below the equilibrium eutectoid temperature (1210 K). Therefore, no endothermic peak from the dissolution of β + Si to α at the eutectoid temperature could be observed. However, if we use an alloy with the same composition which was pre-annealed at 973 K for 5.28×10^4 s, then the DTA curve shows a sharp endothermic peak at the equilibrium eutectoid temperature during the first heating, as shown in Fig. 6b. By the pre-annealing, α has completely decomposed to β + Si and then thus β + Si transformed to α with an endothermic peak. Once the α was formed, it was stable for further cooling or heating stages. The DTA patterns after the first heating were almost the same as those in Fig. 6a.

Fig. 6c shows DTA curves of $Fe_2Si_5$1Mn–1Cu alloy. There are two peaks in the first heating stage. Those are a broad exothermic peak at about 970 K and a large endothermic peak at around 1190 K. On the other hand, only one sharp exothermic peak at about 1110 K was observed during the cooling stage. In the further heating or cooling stages, the patterns were almost the same except the elimination of the first broad exothermic peak, which was observed at the first heating stage.

Fig. 7 shows the X-ray diffraction patterns of specimens which were quenched at A, B and C in Fig. 6c during the DTA measurement. All of α have completely transformed to β and Si in sample A. Sample B shows only α and it means that the above β and Si were transformed to α with a large endothermic peak. The sample C shows only β and Si. Therefore, the α transformed to β and Si with a large exothermic peak.

These results suggest that the exothermic reaction is a reverse reaction of the endothermic reaction. The exothermic reaction occurred with some amount of undercooling. The extent of the undercooling can be evaluated as an index of the stability of α. So in the case of a Cu-free alloy, the undercooling is infinite and α was quite stable. In reality, we can not see any evidence of β formation.

In the lower Cu content alloys, similar patterns were obtained as shown in Fig. 6d–f. The height of the

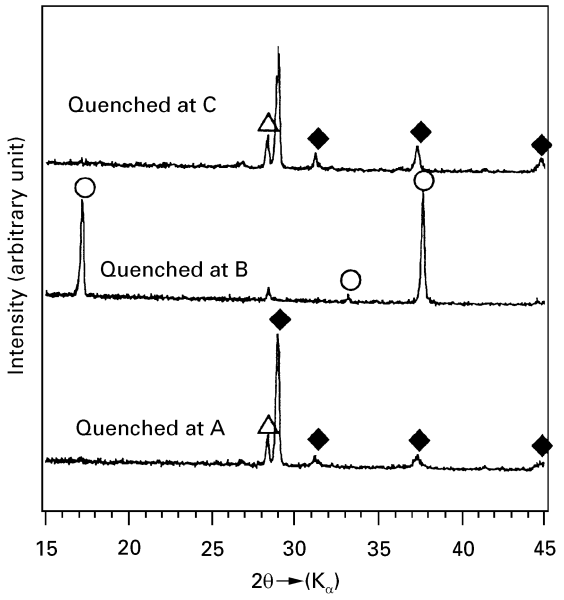

Figure 7 X-ray diffraction patterns of samples quenched at several temperatures during DTA measurements shown in Fig. 6c ($Fe_2Si_5$1Mn alloy). (○) α; (◆) β; (△) Si.

TABLE III Degree of undercooling ($\Delta T = T_{sh} - T_{sc}$) (K) for β-phase formation (T_{sh}: start temperature for endothermic reaction and T_{sc}: start temperature for exothermic reaction as indicated in Fig. 6c)

Alloy	1st			2nd			3rd		
	T_{sh}	T_{sc}	ΔT	T_{sh}	T_{sc}	ΔT	T_{sh}	T_{sc}	ΔT
Fe_2Si_5	–	–	–	–	–	–	–	–	–
Fe_2Si_5–0.1Cu	1231	1082	149	1236	1070	166	1237	1058	179
Fe_2Si_5–0.2Cu	1235	1097	138	1233	1095	138	1233	1094	139
Fe_2Si_5–0.5Cu	1225	1105	120	1226	1103	123	1227	1102	125
Fe_2Si_5–1.0Cu	1231	1112	119	1229	1108	121	1228	1104	124
$Fe_2Si_5$1Mn	–	–	–	–	–	–	–	–	–
$Fe_2Si_5$1Mn–0.1Cu	1212	1020	192	1224	1024	200	1228	1029	199
$Fe_2Si_5$1Mn–0.2Cu	1207	1059	148	1223	1070	153	1223	1068	155
$Fe_2Si_5$1Mn–0.5Cu	1206	1087	119	1221	1089	132	1222	1086	136
$Fe_2Si_5$1Mn–1.0Cu	1206	1104	102	1220	1093	127	1219	1084	135
$Fe_2Si_5$1Co	–	–	–	–	–	–	–	–	–
$Fe_2Si_5$1Co–0.1Cu	1221	1067	154	1225	1066	159	1226	1065	161
$Fe_2Si_5$1Co–0.2Cu	1220	1024	196	1219	1044	175	1219	1044	175
$Fe_2Si_5$1Co–0.5Cu	1205	1058	147	1213	1062	151	1209	1061	148
$Fe_2Si_5$1Co–1.0Cu	1206	1082	124	1215	1064	151	1215	1065	150

exothermic peak became lower with the decrease of Cu content. The temperature difference between endothermic (T_{sh}) and exothermic (T_{sc}) temperatures was defined as undercooling of the decomposition of α. T_{sh} and T_{sc} were imposed in Fig. 6c. The lower undercooling means the higher formation rate of β. Table III shows the summary of the undercooling in various alloys. Cu is effective to decrease the undercooling. The addition of dopant such as Mn or Co significantly stabilized α, especially in low Cu content alloys. The undercooling was almost the same in 0.5 and 1.0 Cu added alloy.

Fig. 8 shows microstructures of $Fe_2Si_5$1Mn–XCu alloys which were cooled to room temperature after DTA measurement. In the case of Cu-free alloys (Fig. 8a, b), we can not see any evidence of the β formation as expected in the DTA curve in Fig. 6a and b. When 1 at % of Cu was added, its structure shows two phase configurations composed of matrix β and the dark precipitates of Si (Fig. 8c). When Cu content decreased to 0.5 at %, then its structure was almost the same as to that of 1 at % Cu alloy. The structure of 0.2 at % Cu alloy became slightly fine and finally it became too fine and it was too difficult to detect Si precipitates in 0.1 at % Cu alloy. These results were also similar to those of Fe_2Si_5–XCu and $Fe_2Si_5$1 Co–XCu alloys. It was clear that Cu was also effective to increase the size of Si.

Fig. 9 shows the variation of X-ray diffraction patterns of various $Fe_2Si_5$1Mn–XCu alloys with isothermal annealing time at 1073 K. In the Cu-free alloy, some amount of α still remained even for 9600 s annealing (Fig. 9a). On the other hand, in 1 at % Cu alloy, a small amount of β was formed only for 120 s

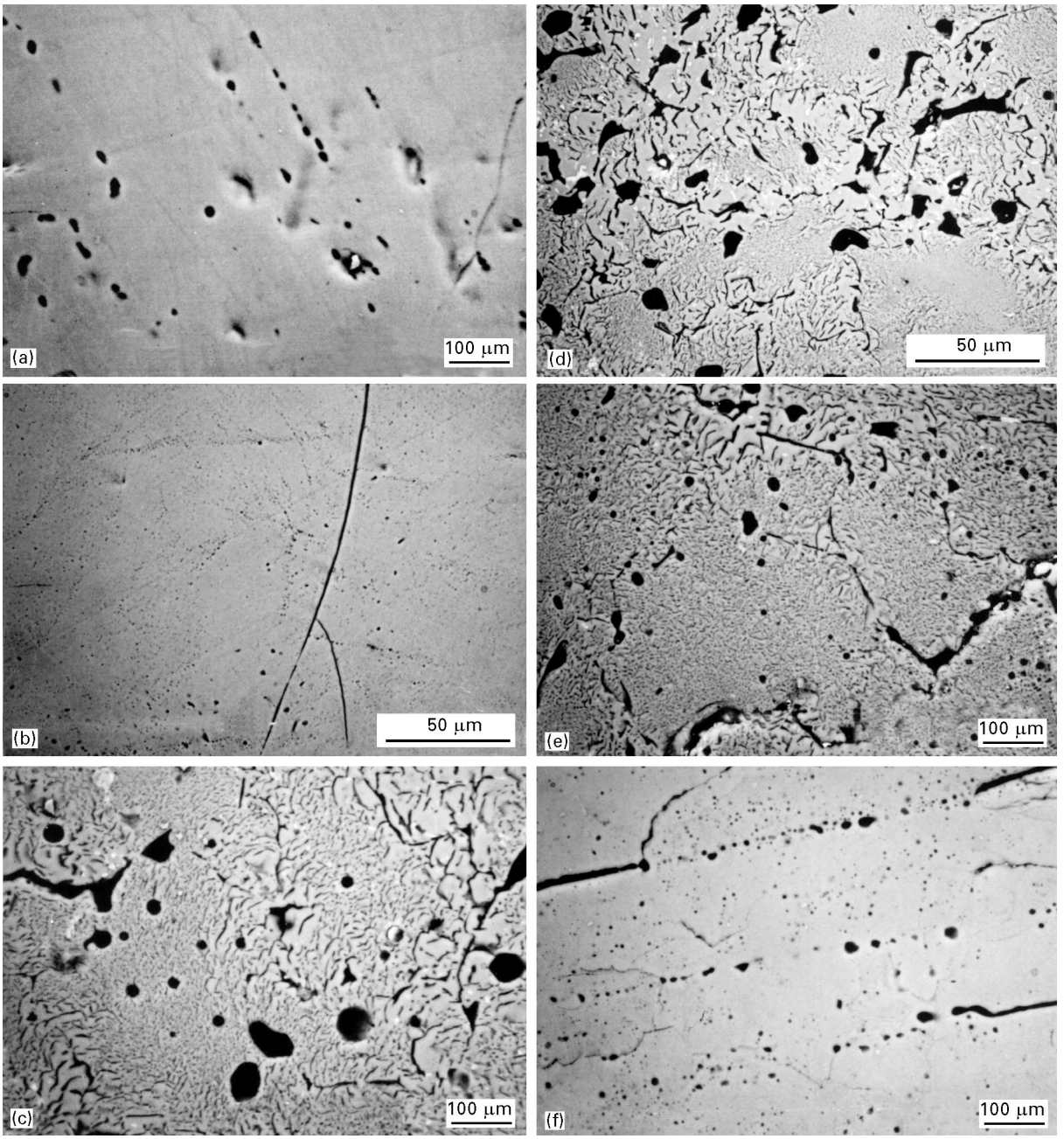

Figure 8 Microstructures of the specimens after DTA measurements in various $Fe_2Si_5$1Mn–XCu alloys: (a) 0 at % Cu; (b) 0 at % Cu (after 5.28×10^4 s at 973 K); (c) 1.0 at % Cu; (d) 0.5 at % Cu; (e) 0.2 at % Cu; (f) 0.1 at % Cu.

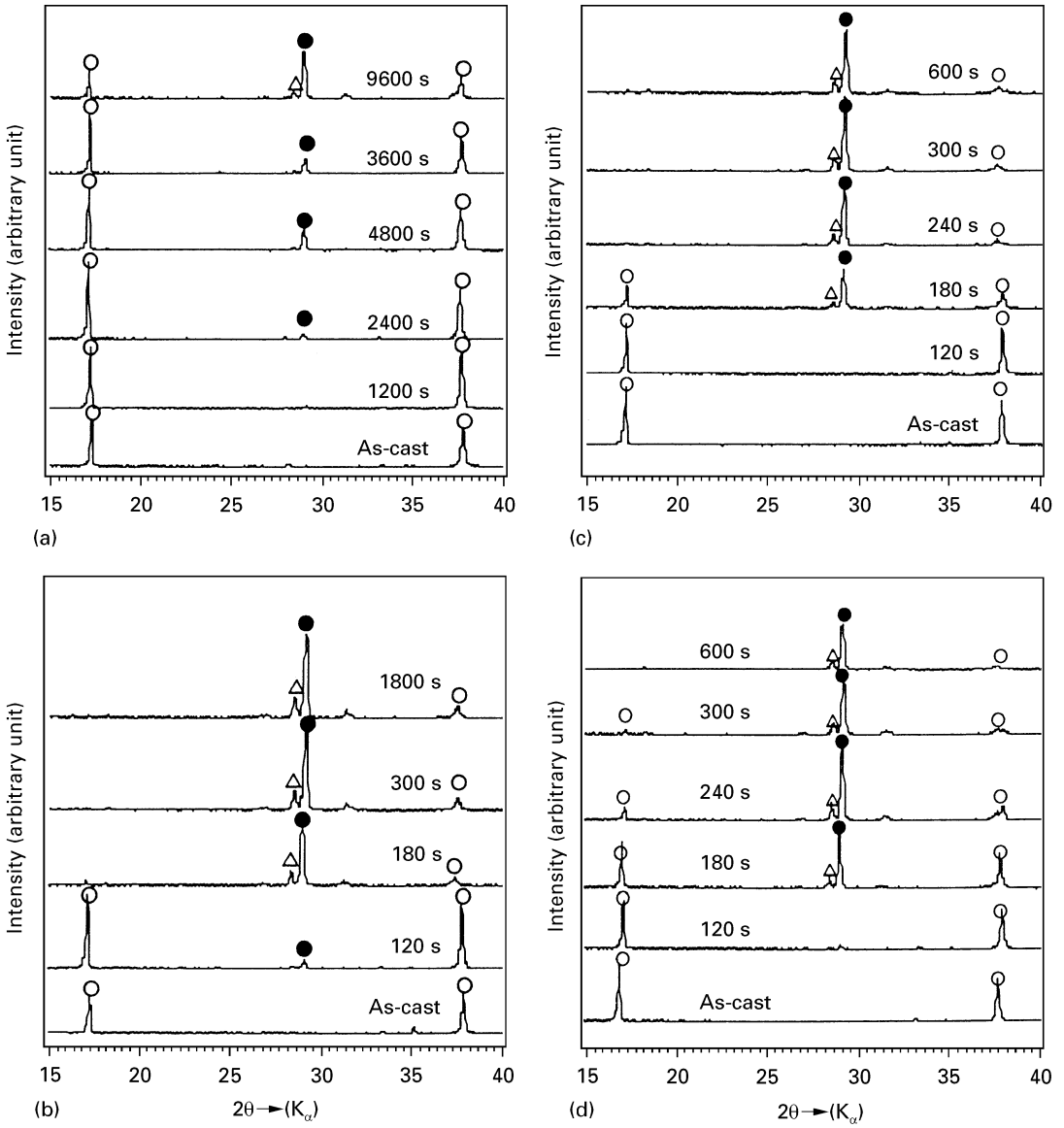

Figure 9 Variation of X-ray diffraction patterns of Fe_2Si_51Mn–XCu alloys (x = (a) 0.0, (b) 0.1, (c) 0.2, (d) 1.0) with annealing time (annealed temp: 1073 K). (○) α; (●) β; (△) Si.

annealing and the reaction completed for 180 s annealing (Fig. 9b). Thus, the effect of Cu on the β formation was drastic. Its effect decreases with decrease of Cu, as shown in Fig. 9b–d. Even in 0.1 at % Cu alloy, its effect was still excellent. All of α completely transformed to β + Si for 300 s annealing.

Fig. 10 shows the variation of X-ray diffraction patterns of Fe_2Si_51Mn–1Cu alloys with annealing temperature. These results show that the β formation rate clearly depends on the annealing temperature. It is fastest in the temperature range of 1073 to 1123 K. However, even at 923 K, α completely decomposed to β + Si within 2400 s annealing for a 1 at % Cu alloy. On the contrary, only 3% of β was formed for 2×10^4 s annealing at 923 K for a Cu-free alloy. Similarly, at 1173 K, 300 s was enough for complete β formation for a 1 at % Cu. Only 9 at % of β was formed for a Cu-free alloy at the same temperature annealing. Fig. 11 shows the effect of Cu content and annealing temperature for β formation rate. The ratio of the formation rate of Cu-added alloy to that of Cu-free alloy is about 50 times at 1073 K and more than 100 times at 973 K.

Fig. 12 shows an example of the bright field image of TEM micrography of Fe_2Si_51Mn–0.1Cu alloy annealed at 1073 K for 600 s. The β contains many planar faults. The white granular particles are Si particles formed by the eutectoid decomposition. These faults are parallel to [0 1 0] direction. From the crystallographic structure of β [8, 9], these faults are stacking faults. We found a different stacking fault model formed by the 1/2 [0 1 0] displacement on the stacking fault plane (1 0 0) [10] to that proposed by Sumida *et al.* [8]. Similar faults were also observed by Hasaka *et al.* [11, 12]. Thus, the β ordinary transformed from α with stacking faults. The crystal structure of β is complicated and it has 48 atoms in a unit cell. For the transformation from α to β, it was probably difficult to perfectly rearrange to a complete unit cell. If the stacking fault on (1 0 0) plane to 1/2 [0 1 0] direction was formed, the unit cell was split to two half unit cells. The above results suggest that it is easier to transform

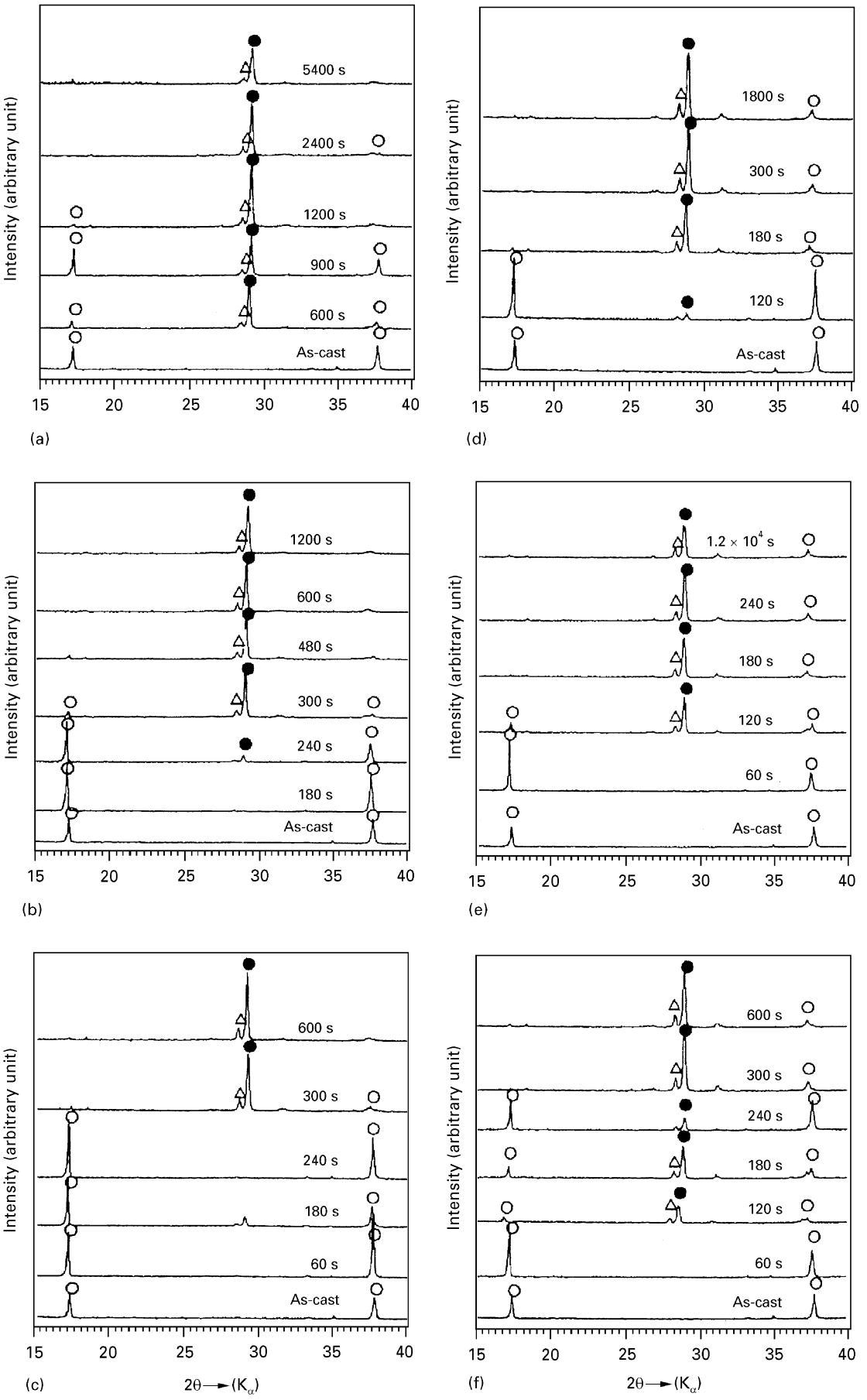

Figure 10 X-ray diffraction patterns of $Fe_2Si_5$1Mn–XCu alloys show effects of annealing temperatures and Cu content on the β formation. (a) 923 K; (b) 973 K; (c) 1023 K; (d) 1073 K; (e) 1123 K; (f) 1173 K. (○) α; (●) β; (△) Si.

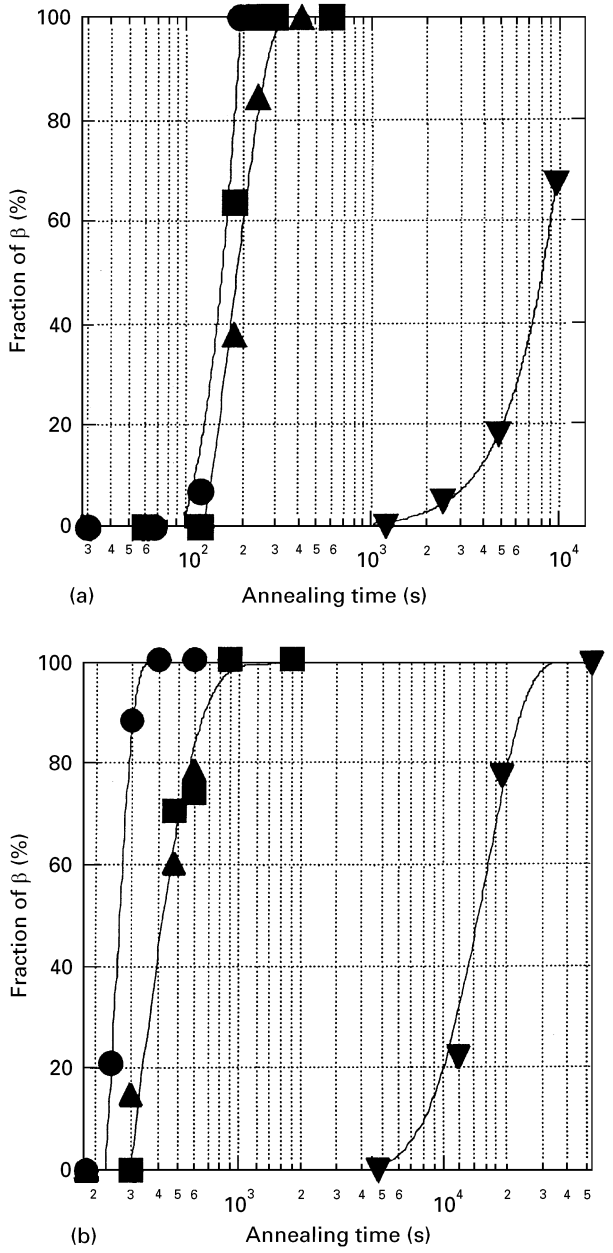

Figure 11 Variation of β fraction with annealing time and temperature shows the effects of Cu on its formation rate. (a) annealed at 1073 K; (b) annealed at 973 K. (●) 1 at %; (■) 0.2 at %; (▲) 0.1 at % (▼) 0 at % Cu.

with stacking faults in comparison with fault-free transformation. Usually, the transformation rate will be enhanced by increase of the diffusion coefficient. However, it is difficult to explain the reason of the drastic acceleration of the β formation only by the increase of diffusion coefficient, especially in case of 0.1 at % addition. We speculate that the reason why the small amount of Cu addition enhanced the β phase formation rate is to decrease this stacking fault energy which acts the drag force for the β phase formation. If the added Cu can segregate on the (1 0 0) plane and decrease the stacking fault energy by decreasing the bonding energy of atoms across the (1 0 0), the drag force for the β formation will be decreased and then the transformation to β will become easy. The detail of the mechanism will be further discussed in another paper [10].

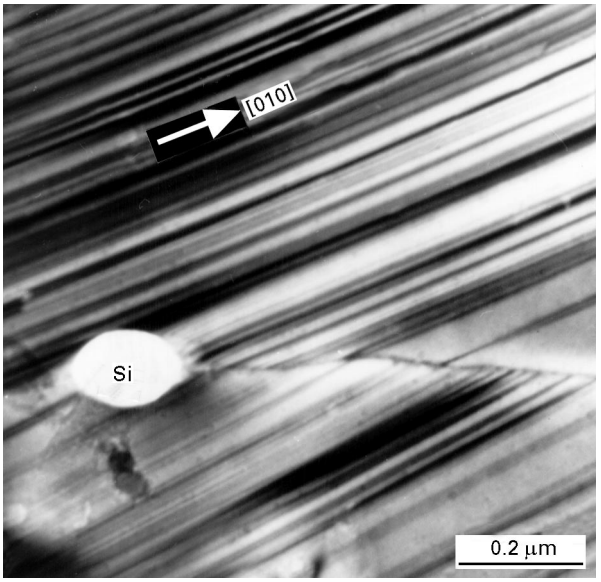

Figure 12 Bright field image of $Fe_2Si_5$1Mn–0.1Cu alloys annealed at 1073 K for 600 s.

4. Conclusions

1. Cu was a quite effective additive for the β phase formation rate in Fe_2Si_5 composition alloy. The effect increases with increase Cu content. At even 0.1 at % addition, its rate increased at least about 50 times greater than that in Cu-free alloy. Its effect was much more remarkable at lower temperature annealing.

2. At 0.1 at % Cu alloy, as-solidified structure was a single phase of α. β was formed only by the eutectoid reaction ($\alpha \rightarrow \beta + Si$) and the size dependence in the peritectoid reaction ($\alpha + \varepsilon \rightarrow \alpha$) in the conventional $FeSi_2$ composition alloy was negligible. It is not necessary to refine the as-solidified structure by using some special techniques such as rapid solidification, mechanical alloying or powder metallurgy. Except for the brittleness, this alloy has a possibility for use at the as-cast state.

3. The additions of Mn or Co as a dopant in Cu added alloy slightly decreased the effect but it was negligibly small.

4. One of the reasons was Cu addition was speculated that Cu decreases the stacking fault energy in α to β transformation.

References

1. U. BIRKHOLTZ and J. SCHELM, *Fiz. Stat. Sol.* **27** (1968) 413.
2. I. NISHIDA, *Phys. Rev. B* **7** (1973) 2710.
3. T. SAKATA and I. NISHIDA, *Bull. Jpn. Inst. Met.* **15** (1976) 1.
4. "Binary alloy phase diagram" edited by T. B. Massalsky (ASM, Metals Park, Ohio, 1986) p. 1108.
5. T. SAKATA, Y. SAKAI, H. YOSHINO, H. FUJII and I. NISHIDA, *J. Less Common Metals* **61** (1978) 301.
6. I. YAMAUCHI, S. UEYAMA and I. OHNAKA, *J. Mater. Sci. Eng.* **15** (1996) 108.
7. I. YAMAUCHI, A. SUGANUMA, T. OKAMOTO and I. OHNAKA, *J. Mater. Sci.* **32** (1997) 4603.
8. N. SUMIDA, T. MISHIMA and H. FUJITA, *J. Jpn. Inst. Met.* **54** (1990) 1302.

9. P. Y. DUSAUSOY, J. *Protas*: *Acta Cryst*. **B27** (1971) 1209.
10. I. YAMAUCHI, T. OKAMATO and I. OHNAKA, *J. Mater. Sci.* submitted.
11. M. HASAKA, T. HARANO, T. MORIMURA and S. KONDO in Proceedings of the 12th International Conference on Thermoelectrics (1993, Yokohama) edited by K. Matuura, p. 316.
12. M. HASAKA, T. MORIMURA, T. HARANO, H. NAKASHIMA and S. KONDO, in Proceedings of the 12th International Conference on Thermoelectrics (1993, Yokohama) edited by K. Matuura, p. 242.

Received 30 July 1996
and accepted 5 August 1997